Deep–Sea Research I 223 (2025) 104534

Contents lists available at ScienceDirect

Deep-Sea Research Part I

journal homepage: www.elsevier.com/locate/dsri

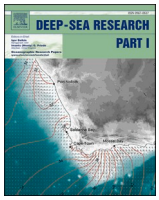

Decadal change in deep-ocean dissolved oxygen in the North Atlantic Ocean and North Pacific Ocean

Henry A. Ruhl [a,*], Christine L. Huffard [a], Monique Messié [a], Thomas P. Connolly [b], Thomas Soltwedel [c], Frank Wenzhöfer [c,d], Rodney J. Johnson [e], Nicholas R. Bates [e,f], Susan Hartman [g], Anita Flohr [g], Edward W. Mawji [g], David M. Karl [h], James Potemra [h], Fernando Santiago-Mandujano [h], Tetjana Ross [i], Kenneth L. Smith [a]

[a] Monterey Bay Aquarium Research Institute, Moss Landing, CA, United States of America
[b] Moss Landing Marine Laboratories, San José State University, Moss Landing, CA, United States of America
[c] Alfred-Wegener-Institute Helmholtz Centre for Polar and Marine Research, Bremerhaven, Germany
[d] HADAL, Department of Biology, University of Southern Denmark, Odense, Denmark
[e] School of Ocean Futures, Julie Ann Wrigley Global Futures Laboratory and College of Global Futures, Arizona State University (ASU), AZ, United States of America
[f] ASU-Bermuda Institute of Ocean Sciences, St. George's, Bermuda
[g] National Oceanography Centre, Southampton, United Kingdom
[h] University of Hawai'i at Mānoa, Honolulu, HI, United States of America
[i] Fisheries and Oceans Canada, Institute of Ocean Sciences, Sidney, BC, Canada

A B S T R A C T

Declining dissolved oxygen concentrations are documented at upper and mid ocean depths, but less is known about the deep ocean. Long time-series measurements of dissolved oxygen analyzed with Winkler titration over several decades reveal regional differences at six stations in the abyssal North Atlantic Ocean and North Pacific Ocean. A significant decline in dissolved oxygen was evident at two stations in the northeast Pacific Ocean at 4000–4200 m depth (Stations PAPA and M). A similar decreasing but insignificant trend was recorded in the Arctic region of the North Atlantic Ocean (HAUSGARTEN). However, there was no significant decrease in dissolved oxygen at two temperate stations in the North Atlantic Ocean (PAP, BATS) and at one tropical station in the central North Pacific Ocean (ALOHA) all at similar depths >4000 m over similar time periods. Continued long time-series observations will be needed to monitor global deep ocean processes and the impact of changing climate. We compare these rare long-term observations with model estimations from historical (1850–2014) and projected (2015–2100) forcing under a continued high greenhouse gas emission scenario.

1. Introduction

Dissolved oxygen primarily enters the ocean at high latitudes in the North Atlantic Ocean and Southern Ocean through surface ventilation. Dissolved oxygen originating in these cold surface waters sinks to abyssal depths and is transported through the deep-ocean basins following global overturning circulation (GOC) pathways (Gordon, 1986; Broecker, 1991; Talley, 2013). This transport can take from 600 to 1500 years (Holzer et al., 2021; Rousselet et al., 2021) ending with upwelling from deep water in the Pacific Ocean and Indian Ocean (Talley, 2013). During this transit from source waters, dissolved oxygen content decreases due to mixing and ventilation change, as well as aerobic respiration by organisms in the water column and on the seafloor (Helm et al., 2011; Schmidtko et al., 2017). This decreasing oxygen in the deep ocean is strongly impacted by climate variability where warming is associated with reduced oxygen solubility and increased stratification that reduces ventilation (Long et al., 2016).

Strong evidence shows that dissolved oxygen is declining in the world ocean (Breitburg et al., 2018; Gregoire et al., 2021). This is especially evident in surface and mid-depth waters. Declines in deeper water have been measured from water samples through 2000 m (Helm et al., 2011). Because of the rarity of time-series measurements below 1000 m, the sparse CTD and bottle data have been combined with statistical modeling to estimate the decline in deep-ocean oxygen (e.g. Sarmiento et al., 1998; Keeling et al., 2010; Schmidtko et al., 2017).

At the long time-series Station M in the Northeast Pacific Ocean, bottom-water dissolved oxygen concentration determined by Winkler titration significantly decreased at 4000–4100 m depth over the past 30 years (Smith et al., 2020). Wind stress, coastal upwelling and sediment community oxygen consumption were significantly inversely correlated

* Corresponding author.
E-mail address: hruhl@mbari.org (H.A. Ruhl).

https://doi.org/10.1016/j.dsr.2025.104534
Received 24 April 2024; Received in revised form 15 May 2025; Accepted 2 June 2025
Available online 16 June 2025

with bottom-water dissolved oxygen concentration (Smith et al., 2022). At the Ocean Station PAPA time-series site, farther north, a nearly 60-year decline in oxygen concentration at depths down to 4000 m has been attributed to changes in ocean ventilation (Cummins and Ross, 2020). Higher than expected interannual variation was also found in deep-water dissolved oxygen at both the Bermuda Atlantic Time-series Study (BATS) and European Station for Time-Series in the Ocean of the Canary Islands (ESTOC) station timeseries sites (Cianca et al., 2013). Such declines are impacting deep-sea ecosystems (Ross et al., 2020). Are these multi-decadal declines in dissolved oxygen concentration in the Northeast Pacific Ocean indicative of other abyssal regions in the world ocean? To address this question, we examined dissolved oxygen concentration determined by Winkler titration from six long time-series abyssal sites in the North Atlantic Ocean and North Pacific Ocean measured at depths >4000 m that span at least several decades (Fig. 1, Table S1, Karl and Lukas, 1996; Soltwedel et al., 2016; Steinberg et al., 2001; Cummins and Ross, 2020; Hartman et al., 2021; Smith et al., 2022). Two inclusive null hypotheses were tested. 1) There is no significant decrease ($p < 0.05$) in measured dissolved oxygen concentration at depths >4000 m on decadal scales in the North Atlantic Ocean and North Pacific Ocean. 2) There is no significant correlation ($p < 0.05$) between measured dissolved oxygen concentration at depths >4000 m and possible satellite-derived surface ocean conditions or regional oceanographic indices on decadal scales in the North Atlantic Ocean and North Pacific Ocean.

Bottom water samples of dissolved oxygen determined with the Winkler technique (Carpenter, 1965; Parsons et al., 1984) were analyzed at each station to provide annual values over the time period spanning 21–33 years from 1989 through 2022 (see Methods Section).

2. Materials and Methods

Bottom water dissolved oxygen concentrations (1989 through 2022) for time-series sites and nearby World Ocean Circulation Experiment (WOCE; Feely et al., 1991; Wong et al., 1994; Johnson et al., 1996; Goyet et al., 1997; Johnson et al., 2003; Feely et al., 2008) and GO-SHIP sites were measured from Winkler titration (Parsons et al., 1984), and either downloaded from a public data repository or acquired through the authors' own access to time-series program data (Dataset S1). Bottom water temperature and salinity measured by CTDs were compiled from these same sources. Data were averaged daily, then yearly.

Satellite monthly time-series were constructed in the vicinity of each station by spatially averaging monthly maps within a 100 km radius circle centered on each station. This radius was found to be useful in several examinations of connections between surface and abyssal seafloor conditions (e.g., Smith et al., 2008; Ruhl et al., 2020). The variables include sea surface temperature (SST), wind stress (WS), Ekman pumping, and chlorophyll concentration (Chl). Sea surface temperature was the Optimum Interpolation SST data (OISST) v2.1 produced by NOAA (Huang et al., 2020). Daily SST on a 0.25° × 0.25° grid were downloaded from https://www.ncei.noaa.gov/products/optimum-interpolation-sst for 1989 onward. Wind speeds were obtained from the Cross-Calibrated Multi-Platform (CCMP) version 2.0 product at 1/4° and 6 h resolution for 1989-onward (Atlas et al., 2011; Wentz et al., 2015; https://www.remss.com/measurements/ccmp/) and averaged daily. Wind stress was calculated following Large and Pond (1981), and Ekman pumping computed from the wind stress on daily time steps (Messié et al., 2009). Monthly Chl concentrations were the OC-CCI version 5.0 product (Sathyendranath et al., 2019, 2021) downloaded from https://www.oceancolour.org/on a 4 km grid. Daily datasets were averaged monthly prior to being averaged spatially (wind stress vectors were averaged monthly prior to computing wind stress magnitude) and then yearly per site.

Modeled dissolved oxygen concentrations for each abyssal time-series location were accessed from the Community Earth System Model version 2 (CESM2) Large Ensemble (Danabasoglu et al., 2020; Rodgers et al., 2021). Fifty ensemble members are analyzed which use forcing with Coupled Model Intercomparison Project 6 (CMIP6) protocols (Eyring et al., 2016) for historical (1850–2014) and projected SSP3-7.0 forcing (i.e. a high greenhouse gas emission scenario under the Shared Socioeconomic Pathway 3, with no additional climate policy; 2015–2100). For each time-series location, monthly-averaged dissolved oxygen concentrations were extracted from the nearest model grid cell and depth level. For comparison with observations, modeled oxygen content per unit mass was calculated using a constant density of 1026 kg/m^3. All trends and statistics are calculated on annual averages of the monthly output.

Data analyses and figure generation were performed in R (R Core Team, 2021) in R Studio (R Studio Team, 2022). Stepwise linear regression between oxygen concentration and environmental variables (Fig. S1–8) was conducted using 'olsrr' (Hebbali and Hebbali, 2017). The large number of climate indices available for comparison to oxygen values from Atlantic Ocean sites was reduced to a maximum of three per site, based on the strength of pairwise Spearman's rank correlations

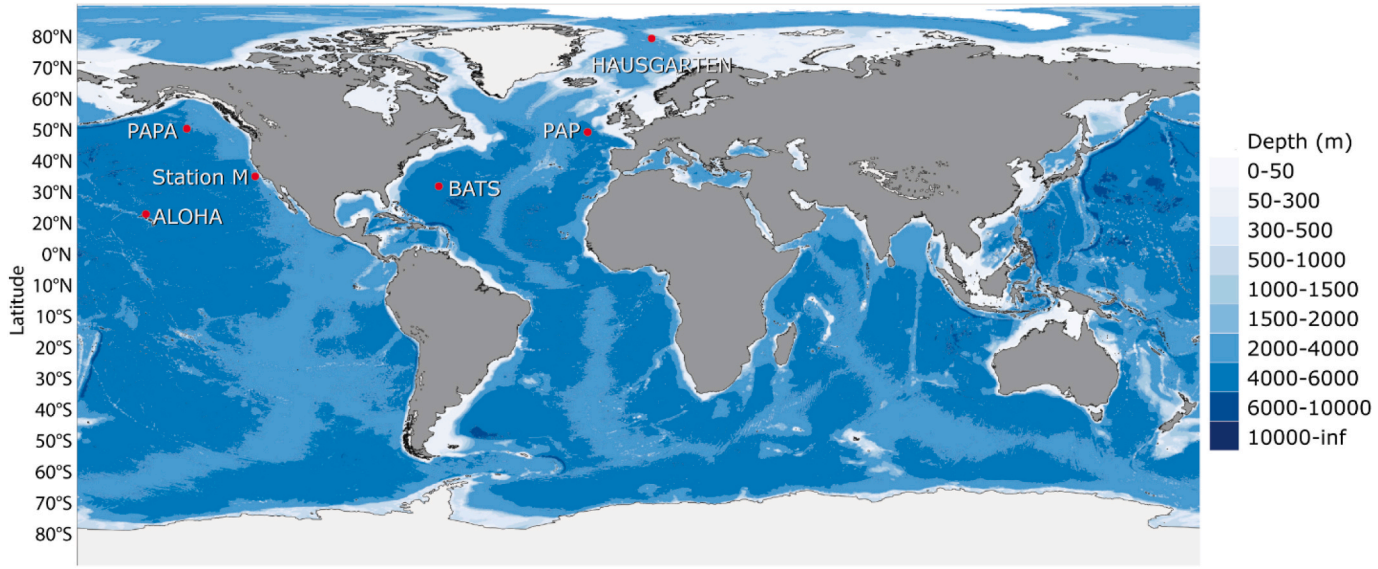

Fig. 1. World chart with long time-series stations marked (HAUSGARTEN, PAP, BATS, ALOHA, PAPA, Station M).

between oxygen values and each Atlantic Ocean climate index. The Breusch-Pagan Lagrange Multiplier test (Breusch and Pagan, 1979) was used to confirm the lack of model heteroscedasticity. The top performing models with two, three and four independent variables respectively are reported, as determined by adjusted R^2 values. The data on which this article is based are available in Smith et al. (submitted here).

3. Results

3.1. North Atlantic Ocean stations

3.1.1. HAUSGARTEN

Annual dissolved oxygen content at this North Atlantic Ocean station

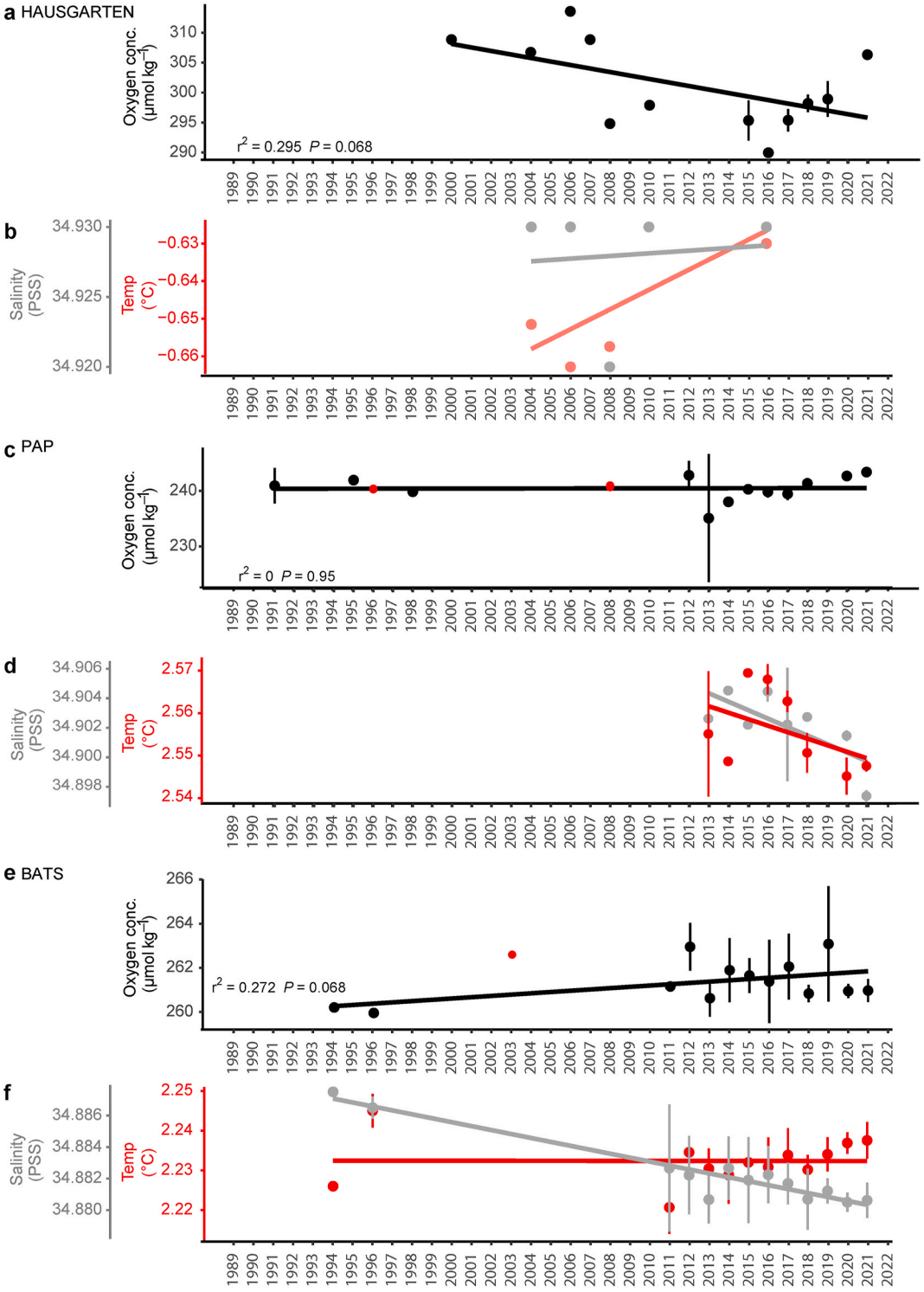

Fig. 2. Time-series of abyssal bottom water oxygen concentration, temperature and salinity including standard deviation bars from 1989 through 2022 at three stations in the North Atlantic Ocean. (a–b) – HAUSGARTEN with measurements at 4000–4100 m depth, (c–d) – PAP measurements at ≥ 4500m depth, (e–f) – BATS measurements between 4300 and 4550 m depth (WOCE and GO-SHIP oxygen values in red). Error bars = standard deviation, where there are sometimes not enough samples for this to be calculated, hence no bar. (For interpretation of the references to colour in this figure legend, the reader is referred to the Web version of this article.)

at 4000–4100m depth in the Arctic region decreased from a high of 313.6 to 289.9 μmol O_2 kg^{-1}, with a mean of 301.2 ± 7.3 μmol O_2 kg^{-1} and a decreasing but insignificant trend (p = 0.068) over the 21-year time-series (Fig. 2A; Table S1). This station would be expected to have high surface ventilation extending to abyssal depths based on the global overturning circulation model (e.g., Talley, 2013) and the low bottom temperature at HAUSGARTEN supports such an exchange (Fig. 2B).

3.1.2. *Porcupine abyssal plain (PAP)*

There was no significant trend (p = 0.95) in dissolved oxygen at this Northeast Atlantic Ocean station >4500 m depth from 1991 through 2021 (Fig. 2C; Table S1). The highest oxygen measurement was 243.4 μmol O_2 kg^{-1} in 2021 and a low of 235.1 μmol O_2 kg^{-1} in 2013 with a mean of 240.5 ± 2.3 μmol O_2 kg^{-1} over the time-series. Dissolved oxygen measurements conducted during World Ocean Circulation Experiment (WOCE) and Global Ocean Ship-based Hydrographic

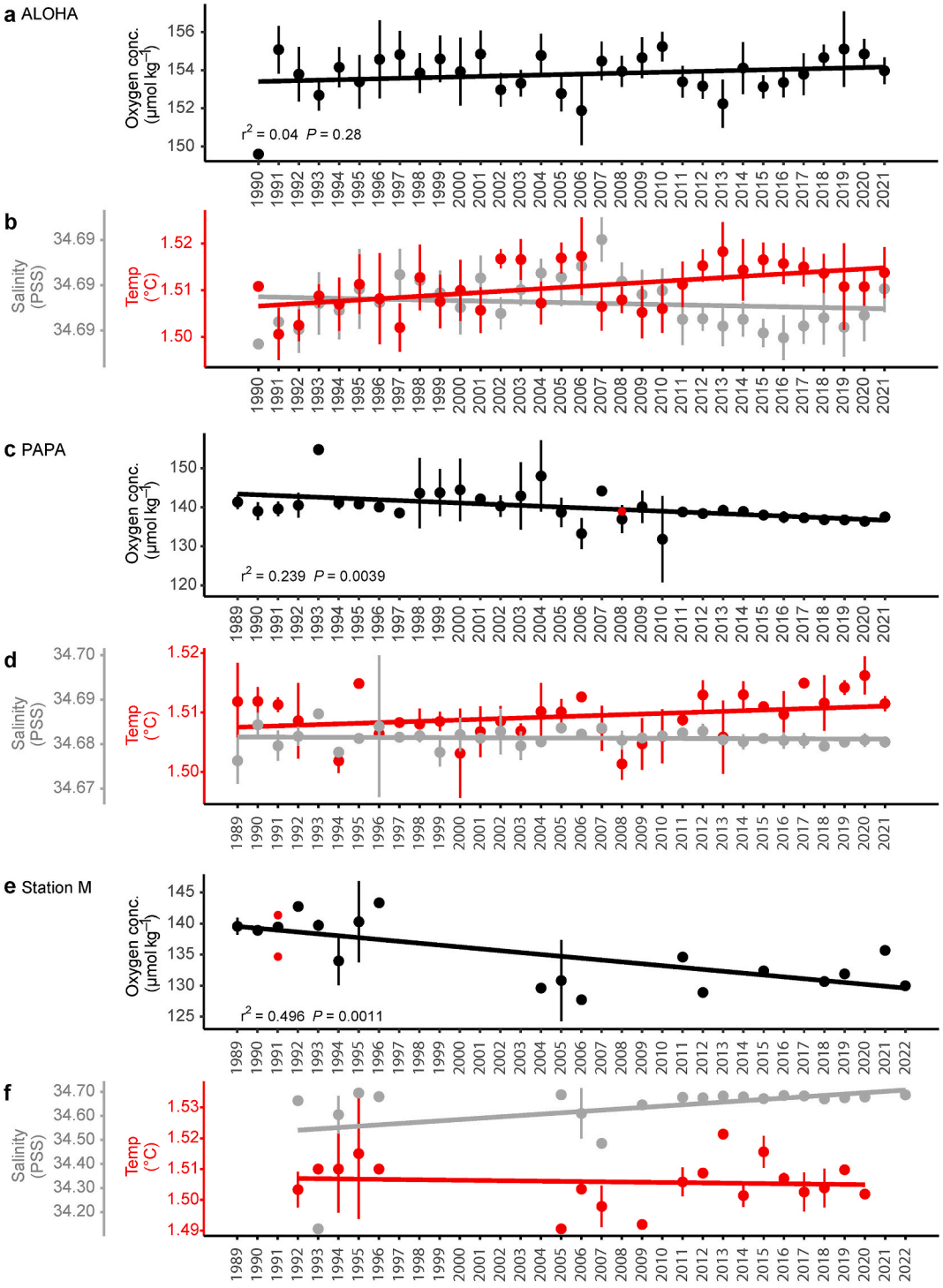

Fig. 3. Time-series of abyssal bottom water oxygen concentration, temperature and salinity from 1989 through 2022 at six stations in the North Pacific Ocean (a–b) - ALOHA measurements at > 4620 m depth, (c–d) - PAPA measurements at > 3880 m, (e–f) - Station M measurements between 4000 and 4100 m depth (WOCE and GO-SHIP oxygen values in red). Error bars = standard deviation. (For interpretation of the references to colour in this figure legend, the reader is referred to the Web version of this article.)

Investigations Program (GO-SHIP) (red dots) at similar depths were consistent with the PAP time-series data.

3.1.3. Bermuda atlantic time-series study (BATS)

Dissolved oxygen at this Northwest Atlantic Ocean station between 4300 and 4550 m depth exhibited an increasing but insignificant trend ($p = 0.06$) from 1994 through 2021 (Fig. 2E; Table S1). There was a narrow range of dissolved oxygen over the time-series from a low of 260.0 μmol O_2 kg^{-1} in 1994 to a high of 263.1 μmol O_2 kg^{-1} in 2019 with an overall mean of 261.4 ± 1.0 μmol O_2 kg^{-1}. Ship-based measurement of dissolved oxygen (red dot) from the GO-SHIP program at a similar depth within the vicinity of BATS was 262.5 μmol O_2 kg^{-1}, toward the high end of the range taken in 2003.

3.2. North Pacific Ocean stations

3.2.1. A long-term oligotrophic habitat assessment - ALOHA

This North Pacific Ocean station in the oligotrophic central gyre exhibited a consistent dissolved oxygen concentration below 4620 m depth between 149.6 and 155.2 μmol O_2 kg^{-1} with a mean of 153.8 ± 1.2 μmol O_2 kg^{-1} (Fig. 3A; Table S1). The narrow range of oxygen values indicates no significant change ($p = 0.28$) from 1991 through 2021. There were no WOCE or GO-SHIP measurements of dissolved oxygen near the bottom at abyssal depths in the vicinity of ALOHA during this time-series. However, all ALOHA measurements are considered WOCE GO-SHIP equivalents.

3.2.2. A long-term oligotrophic habitat assessment - PAPA

Dissolved oxygen at this subarctic Northeast Pacific Ocean station >3880 m showed a significant decline ($p = 0.012$) from 1989 through 2021 (Fig. 3C; Table S1). Values ranged from a high of 154.7 μmol O_2 kg^{-1} in 1999 to a low of 131.8 μmol O_2 kg^{-1} in 2010 with a mean of 140.0 ± 4.2 μmol O_2 kg^{-1} over the 32-year period. A WOCE/GO-SHIP station occupied within the vicinity of PAPA at similar depth reported oxygen measurements in 2008 that fell along the decreasing trend line (Fig. 3C, red dot). Declining dissolved oxygen to deep depths (~2000 m) is well documented at this station over six decades (Cummins and Ross, 2020).

3.2.3. A long-term oligotrophic habitat assessment - Station M

This Northeast Pacific Ocean station beneath the California Upwelling system off central California showed a significant decline ($p = 0.0011$) of dissolved oxygen between 4000 and 4100 m depth. A WOCE station occupied in the vicinity of Station M at similar depth reported oxygen measurements in 1991 (Goyet et al., 1997) similar to those measured at the same year (Smith et al., 2022). There was a high of 143.3 μmol O_2 kg^{-1} in the early 1990's down to 127.6 μmol O_2 kg^{-1} with a mean of 134.9 ± 5.1 μmol O_2 kg^{-1} over the 33-year study period (Fig. 3E; Table S1). There was a significant inverse correlation between abyssal dissolved oxygen and coastal upwelling at Station M (Smith et al., 2022).

3.3. Comparison of stations with global overturning circulation (GOC) and model concepts

We qualitatively compared the bottom water oxygen data at the six time-series stations with respect to a conceptual model of meridional overturning circulation (Talley, 2013). In this model, deep-water formation in the North Atlantic Ocean (North Atlantic Deep Water, NADW) occurs near the HAUSGARTEN site. The NADW then travels south along the North America coast, towards BATS. The PAP site, located on the eastern side of the basin, appears to be outside of the NADW path and thus likely within older, less oxygenated deep waters despite being located at an intermediate latitude between HAUSGARTEN and BATS. All North Pacific Ocean sites are located far from deep-water formation and are expected to be the least ventilated.

3.3.1. North Atlantic Ocean

None of the three North Atlantic Ocean deep-sea stations exhibited a significant decline in dissolved oxygen over a period up to three decades. The highest dissolved oxygen was at the HAUSGARTEN site (4000–4100 m) in the Arctic region of the North Atlantic Ocean with a mean concentration of 301.2 μmol O_2 kg^{-1}. This deep Arctic station would be expected to have high oxygen concentration from surface ventilation extending to abyssal depths, based on the global overturning circulation model indicating deep-water formation in the region (e.g., Talley, 2013). The high dissolved oxygen at HAUSGARTEN over the past 21 years did exhibit an oscillating but decreasing trend with increasing bottom temperature (Fig. 2A and B). Oxygen solubility values calculated from potential temperature and salinity are stable through time within 1 μmol O_2 kg^{-1} at all three North Atlantic Ocean stations (not shown), indicating that oxygen variability is not driven by temperature. The abyssal bottom water oxygen concentrations at the two other North Atlantic Ocean stations farther south are substantially lower than those at HAUSGARTEN. At the subtropical North Atlantic Ocean station, BATS, it is 39.8 μmol O_2 kg^{-1} lower while at the boreal station, PAP, it is 60.7 μmol O_2 kg^{-1} lower than at HAUSGARTEN. Bottom water temperature and salinity properties fall within the range of values for both the warmer and higher salinity North Atlantic Deep Water (NADW) and the colder less saline Antarctic Bottom Water (AABW) (Fig. 2D and F). Although NADW dominates the bottom water in the North Atlantic Ocean, a small fraction of AABW reaches the subtropical western North Atlantic Ocean where BATS is located (Johnson, 2008). The mean apparent oxygen utilization (AOU) is ~18 μmol kg^{-1} higher at PAP compared to BATS, indicating that the differences in mean O_2 are primarily due to biological utilization rather than temperature differences. In the northeast Atlantic Ocean near PAP, deep water generally flows southward along the Mid-Atlantic Ridge and northward along the eastern boundary (Dickson et al., 1985). Regionally within the northeast Atlantic Ocean, AOU in near-bottom water increases to the north towards PAP, consistent with biological utilization in the northward part of this deep-cyclonic recirculation (van Aken, 2000).

3.3.2. North Pacific Ocean

All three stations in the North Pacific Ocean had lower dissolved oxygen concentrations below 4000 m depth than those in the North Atlantic Ocean by almost 100 μmol O_2 kg^{-1} (Table S1). Dissolved oxygen at Station ALOHA in the central gyre was the highest at 153.9 μmol O_2 kg^{-1} exhibiting no long-term change. Farther east, both Station M and PAPA have a similar dissolved oxygen content, which has significantly decreased over the past 32-year period, most notably at Station M. The decline in bottom water dissolved oxygen at Station M has been inversely correlated with coastal upwelling (Smith et al., 2022). PAPA, farther offshore to the northwest is probably influenced by the enrichment of productivity in the Alaskan gyre, contributing increased fluxes of organic carbon to abyssal waters and consuming dissolved oxygen. Strong stratification in the North Pacific Ocean inhibits deep-water formation and limits the influence of surface ventilation to a shallow overturning cell (Talley, 2013). Abyssal waters in the North Pacific Ocean are primarily composed of Antarctic Bottom Water (Johnson, 2008). Temperature and salinity of the bottom waters are similar at all three stations (Fig. 3B–D, F) and fall within the range of values for Antarctic Bottom Water (0.8–2°C; 34.6 to 34.7 psμ; e.g., Hogg et al., 1982).

Long term declines in the ensemble-averaged dissolved oxygen concentrations in CESM 2 are evident at the Pacific Ocean sites, while long-term variability is more complicated at the Atlantic Ocean sites (Fig. 4). In the Pacific Ocean, the rate of oxygen decline is faster in the projected forcing period (2015–2100) than the historical period (1850–2014) at all three sites. However, the model projected annual rates of decline at PAPA (−0.0063 μmol kg^{-1}) and Station M (0.0055 μmol kg^{-1}) are still 1-2 orders of magnitude smaller than the observed trends at those locations (Fig. 5, Smith et al., 2020). The modeled

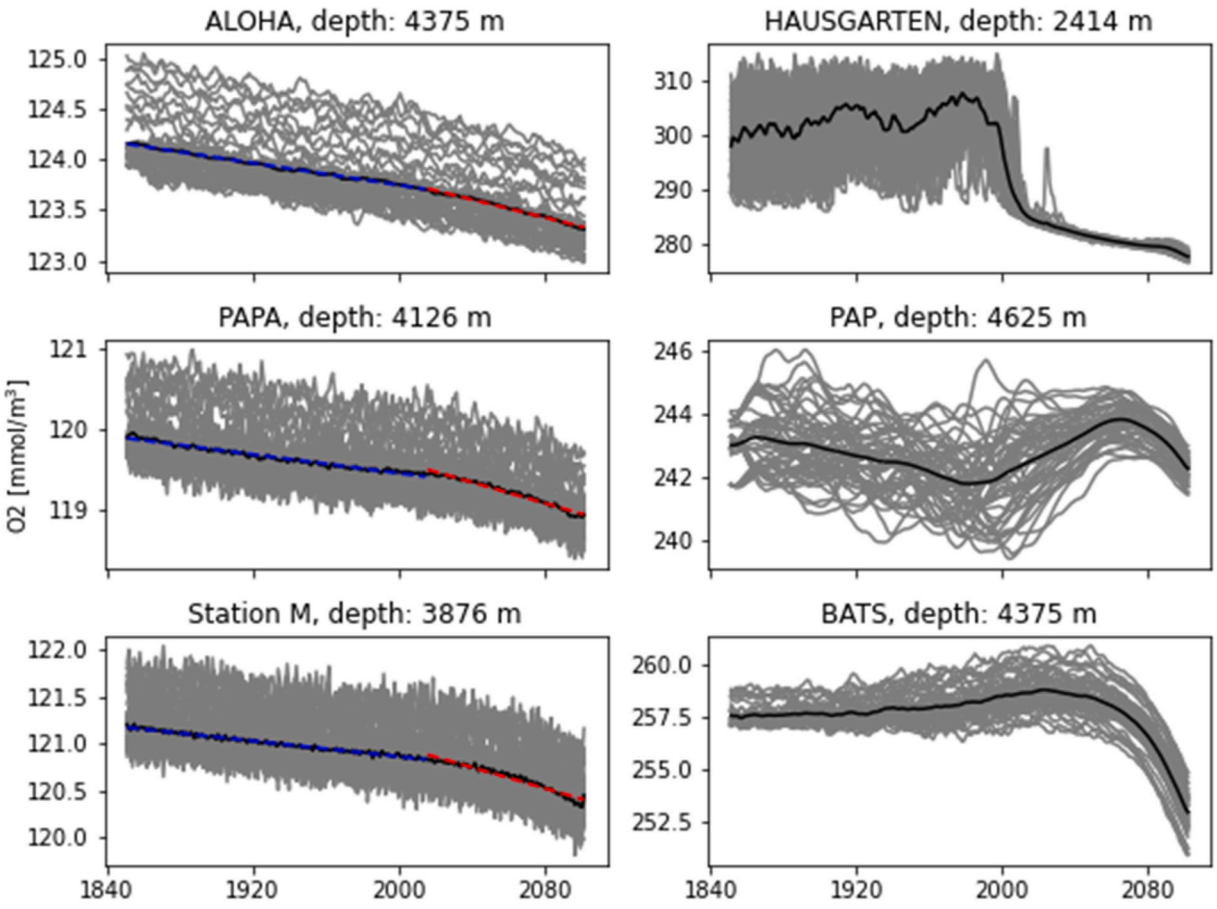

Fig. 4. Modeled dissolved oxygen concentrations from the CESM2 Large Ensemble from each of the abyssal time-series locations. Gray lines represent monthly means from 50 individual ensemble members. Black lines represent ensemble means. At the Pacific Ocean site locations where long-term declines are evident throughout the time-series (left panels), linear trend lines are shown for the historical forcing period (1850–2014, blue) and projected forcing period (2015–2100). (For interpretation of the references to colour in this figure legend, the reader is referred to the Web version of this article.)

interannual variability in the historical period, calculated as the mean of the individual ensemble standard deviations, is also smaller than the observed variability (Fig. 5, Table S1) at all sites except for HAUSGARTEN in the Fram Strait (model SD = 7.37 μmol kg^{-1}). The model output at this location is from much shallower in the water column (~2400 m) than the observations (>4000 m) due to smoothing of the complex regional bathymetry in the coarse model grid, but shows a dramatic reduction in the mean and variability starting in the early 2000's This projected oxygen decline in the Fram Strait corresponds with an increase in apparent oxygen utilization (AOU) but not temperature below the main pycnocline (not shown), suggesting that changes in upstream primary productivity and/or reduced ventilation of abyssal water masses may be explanatory. By the tail end of the model time-series (2070–2100), the trend and variability are similar at all of the Atlantic Ocean sites (Fig. 4). The projected changes highlight the value of continued long-term observations of the abyssal ocean. However, further investigation is warranted. Overall, the weaker interannual variability in modeled dissolved oxygen concentrations indicates that more progress is needed in accurately representing the complex processes that govern carbon export from the surface to the deep ocean.

3.4. Comparison of surface ocean conditions and climate indices with bottom water dissolved oxygen from six stations

While most abyssal waters have not ventilated with the surface ocean for potentially decades to millennia, recently observed changes in overturning circulations speed and direction could relate to variations in abyssal oxygen concentration at some locations. For example, the Atlantic Meridional Overturning Circulation (AMOC) has inter- and intra-annual scale variations and occasional directional reversals that relate to climatic oscillations, with potential for long-term change in the future (Srokosz and Bryden, 2015; Germe et al., 2022). Pelagic-benthic coupling of sinking particulate organic carbon (POC) fluxes from the surface to abyss has also been linked to changes in sediment community oxygen consumption (SCOC) over daily and longer timescales (Ruhl et al., 2008; Smith et al., 2018).

Four satellite-derived parameters representing surface conditions over the duration of the six time-series station oxygen datasets were calculated annually [sea surface temperature (SST), surface wind stress (WS), Ekman pumping (EP), and Chl (Figs. S1–6; Table S2)]. These four parameters were considered as possibly influencing deep-ocean oxygen concentrations through changing organic carbon fluxes from the surface ocean; if non-local surface fluxes dominate the abyssal signal this correlation with local surface condition will be weak. The lowest SSTs were found at the two northernmost stations in the Arctic region of the North Atlantic Ocean (HAUSGARTEN, mean = 2.07 ± 0.48°C) and subarctic North Pacific Ocean (PAPA, mean = 8.87 ± 0.7°C) with reduced seasonal variability especially at HAUSGARTEN. The highest SSTs occurred at the two subtropical stations in the Northwest Atlantic Ocean (BATS, mean = 23.55 ± 0.42°C) and central North Pacific Ocean (ALOHA, mean = 24.81 ± 0.47°C). Surface wind stress (WS) showed limited variability between all six stations with the highest being recorded in the Northeast Atlantic Ocean (PAP, 0.08 ± 0.01) and lowest in the Northwest Atlantic Ocean (BATS, 0.04 ± 0.01). Ekman pumping (EP) was highest in the Northeast Atlantic (PAP, 0.65 ± 0.26) and lowest in the Arctic region of the North Atlantic Ocean (HAUSGARTEN, −1.54 ±

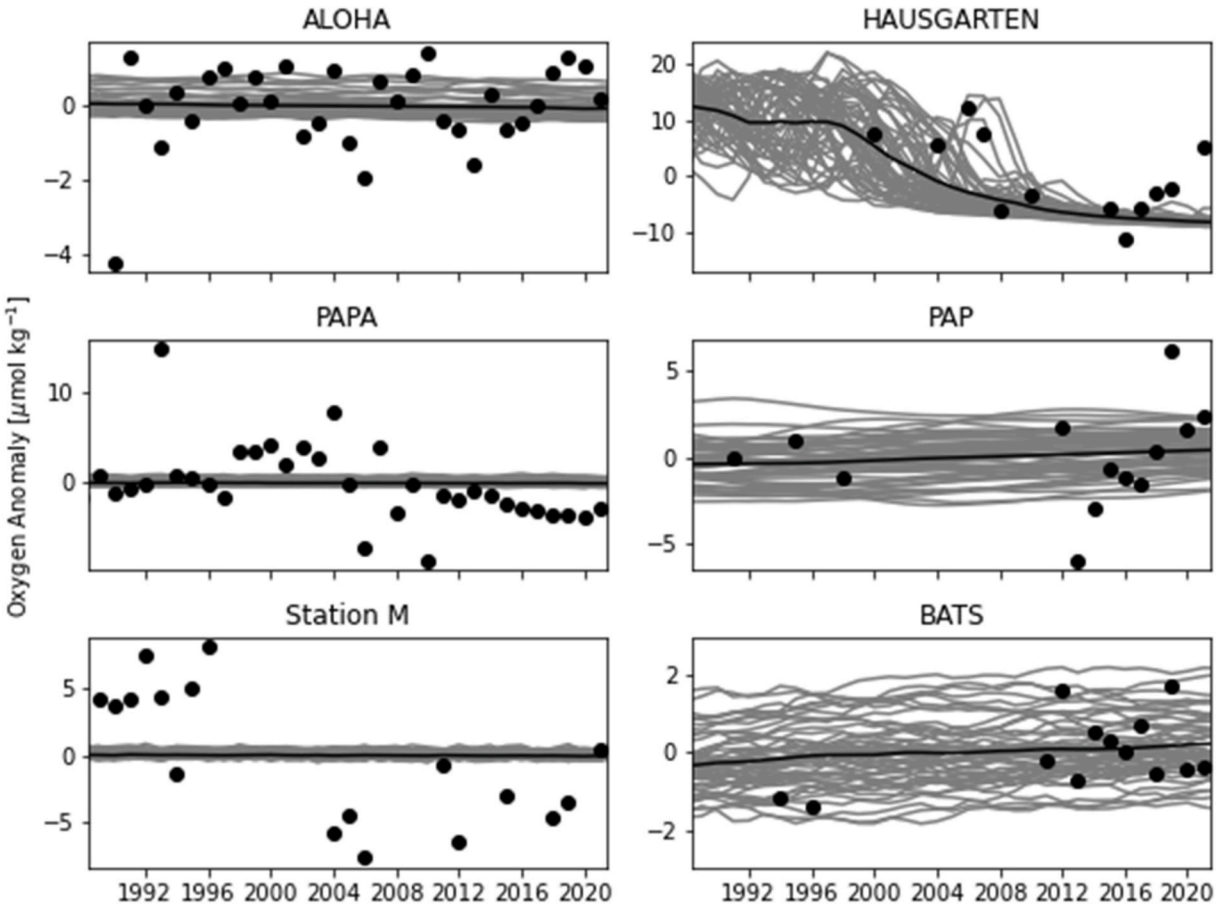

Fig. 5. Dissolved oxygen anomalies from observations and CESM2 Large Ensemble model runs, with mean values from the period 1989–2020 removed. Black circles represent anomalies calculated from the annual averages of the observations. Lines represent anomalies calculated from monthly means from the ensemble members (gray), and the ensemble means (black).

1.16). Surface Chl ranged from a high in the Arctic region of the North Atlantic Ocean (HAUSGARTEN, 1.07 ± 0.21 mg m^{-3}) and Northeast Pacific Ocean (M, 0.45 ± 0.09 mg m^{-3}) to lows in the subtropical Northwest Atlantic Ocean (BATS, 0.10 ± 0.01 mg m^{-3}) and subtropical central North Pacific Ocean (ALOHA, 0.08 ± 0.00 mg m^{-3}).

A stepwise linear regression was applied using the four annually calculated parameters derived from satellite data and six basin-scale ocean indices to distinguish possible correlations with bottom water oxygen at each time-series station (Table S3). When using ordinary least squares approaches (such as stepwise linear regression), R^2 can be considered 1 minus the variance unexplained, and can be negative (Nakagawa and Schielzeth, 2013). In the Arctic region of the North Atlantic Ocean (HAUSGARTEN), the variability of bottom water dissolved oxygen was more strongly correlated with WS, and the Atlantic Multidecadal Oscillation (AMO, Enfield et al., 2001) index, which in combination accounted for 37 % ($p = 0.04$). The principal variables shifted at PAP in the Northeast Atlantic Ocean to EP, Chl and the Atlantic Meridional Mode (AMM; Chiang and Vimont, 2004) covarying with 59 % of the variability in dissolved oxygen ($p = 0.04$). In the Northwest Atlantic Ocean at BATS, the primary covariants with bottom water dissolved oxygen included WS, Chl, the Atlantic Meridional Overturning (AMO) and AMOC indices together accounting for 80 % ($p = 0.03$). For the three North Atlantic Ocean stations, the physical parameters of SST, WS and Chl combined with the AMO, AMOC, and Antarctic Oscillation (AAO) indices were the primary covariants with bottom water dissolved oxygen.

Ekman pumping (EP), Chl, Pacific Decadal Oscillation (PDO; Mantua et al., 1997), North Pacific Gyre Oscillation (NPGO, Di Lorenzo et al., 2008) and the Multivariate ENSO index (MEI; Wolter and Timlin, 1993) were the principal covariants with the abyssal dissolved oxygen concentration at three stations, ALOHA, PAPA and M, in the central and eastern North Pacific Ocean (Table S3). Bottom water dissolved oxygen at ALOHA in the central gyre was correlated with EP and the NPGO index accounting for a combined 7 % of the variability ($p = 0.97$). At Station M in the Northeast Pacific Ocean influenced by the California Current Upwelling, three conditions, SST, EP and Chl, along with the MEI index, together covaried with 79 % of the variability in bottom water dissolved oxygen ($p = 0.03$). PAPA in the Alaskan gyre gave different results based on regression analysis. The closest factors correlating with bottom water dissolved oxygen were EP, WS, Chl and the NPGO ($R^2 = 0.26$; $p = 0.04$; Table S3).

3.5. *Test of two null hypotheses*

Findings based on six abyssal time-series in the northern hemisphere highlight variability in trends in deep-ocean oxygen concentrations. A significant decline in dissolved oxygen was evident in the Northeast Pacific Ocean at Station M and PAPA over the past 32–33 years. This could be related in part to increasing eutrophic conditions in overlying surface waters (Smith et al., 2022) or multi-decadal variability and changes in overturning circulation (Garcia-Soto et al., 2021). However, there may also be longer-term variability of deep-ocean oxygen concentrations at play; e.g. Schmidtko et al. (2017) show no model-estimated trend at the 60-year scale in the deep (3000 m) North Pacific Ocean. Given the age of the deep water, estimated to be > 1000 years, the decreased oxygen could be related to changes in the distant past (Cummins and Ross, 2020), but is more likely due to changes in circulation. There was no significant decline in dissolved oxygen at the

other stations, however.

Three stations in the North Atlantic Ocean (HAUSGARTEN, PAP, BATS) and one station in central North Pacific Ocean (ALOHA) showed no significant decline over the past 21–32 years. These site-specific results are in line with geographic variation in estimated oxygen declines in the deep ocean (Schmidtko et al., 2017). Considering these regional differences, the null hypothesis (#1) that there is no significant decline in abyssal ocean dissolved oxygen concentration can be accepted for the global ocean on a 30-year time scale, while acknowledging the trends in the Northeast Pacific Ocean were declining and significant.

As surface oceanographic variables and climate indices were correlated with bottom oxygen only in some regions and different sets of variables were important in different regions, this empirical search for an inclusive conceptual model to explain the time-series variability in abyssal dissolved oxygen yielded no definitive answer. Wind stress (WS) was a significant predictor of dissolved oxygen concentration at four stations, three in the Atlantic Ocean and one in the Pacific Ocean (Table S3). Chlorophyll concentration also correlated with oxygen concentration at four sites – two in the Pacific Ocean, and two in the Atlantic Ocean. Regional oceanographic indices were locally important, with at least one identified as a predictor in the top performing model at each station. Given these results, the null hypothesis (#2) that there is no significant correlation between measured dissolved oxygen concentration at depths >4000 m and satellite-derived surface ocean conditions or regional oceanographic indices on decadal scales in the North Atlantic Ocean and North Pacific Ocean can be accepted.

4. Conclusions

There is no consistent trend of decreasing dissolved oxygen concentration at abyssal depths across the six deep-sea time-series stations in the North Atlantic Ocean and North Pacific Ocean. None of the three North Atlantic Ocean time-series stations, HAUSGARTEN, PAP and BATS, exhibited a significant decline in dissolved oxygen over a period up to three decades. Similarly, in the North Pacific Ocean central gyre, ALOHA, there was no significant decline in dissolved oxygen at abyssal depths over three decades. In contrast, the oxygen concentration at > 4000 m depth at two time-series stations in the Northeast Pacific Ocean, PAPA and Station M, showed a significant decline ($p < 0.02$) from 1989 through 2022.

There is a trend of decreasing oxygen at depths >4000 m at locations farther from sources of surface ventilation in the Arctic region of the North Atlantic Ocean and Southern Ocean following the global overturning circulation (GOC) model (e.g., Talley, 2013). The highest oxygen concentration was recorded at HAUSGARTEN in the Arctic region of the North Atlantic Ocean, a source of surface ventilation. There is less dissolved oxygen at the Northeast and Northwest Atlantic Ocean stations, which are farther from the sources of deep-water formation and ventilation. Bottom water dissolved oxygen concentration is much smaller at the North Pacific Ocean stations >100 μmol kg^{-1} less than the North Atlantic Ocean, being higher in the central gyre than the northeast. Abyssal water at 4000 m depth in the North Pacific Ocean flows eastward across the subtropical North Pacific Ocean, past ALOHA towards Station M, and northward along the eastern boundary (Reid, 1997). The dissolved oxygen concentrations at abyssal depths measured at the six time-series stations support the flow trajectory of the global conceptual overturning circulation (GOC) model.

Bottom water dissolved oxygen concentration at five of the six time-series stations in the North Atlantic Ocean (HAUSGARTEN, PAP, BATS) and North Pacific Ocean (PAPA, Station M) correlated with a combination of satellite-derived surface ocean conditions and basin-scale indices averaged annually.

The comparison of the *in situ* observations with the ocean model estimates of change revealed both differences and similarities that punctuate the importance of long term observations to understand change. Observations and models have important differences in terms of measurement error of observations and inherent mechanistic limits of change in models. The differences across the stations in coherent variances between the anomalies of the observations vs. the models over time, for example, reveal an ongoing gap in understanding abyssal biogeochemistry.

CRediT authorship contribution statement

Henry A. Ruhl: Writing – review & editing, Visualization, Validation, Supervision, Project administration, Methodology, Investigation, Formal analysis, Data curation, Conceptualization. **Christine L. Huffard:** Writing – review & editing, Visualization, Software, Project administration, Methodology, Formal analysis, Data curation. **Monique Messié:** Writing – review & editing, Visualization, Methodology, Formal analysis. **Thomas P. Connolly:** Writing – review & editing, Visualization, Validation, Software, Methodology, Investigation, Formal analysis. **Thomas Soltwedel:** Writing – review & editing, Validation, Data curation. **Frank Wenzhöfer:** Writing – review & editing, Validation, Data curation. **Rodney J. Johnson:** Writing – review & editing, Validation, Data curation. **Nicholas R. Bates:** Writing – review & editing, Validation, Data curation. **Susan Hartman:** Writing – review & editing, Validation, Data curation. **Anita Flohr:** Writing – review & editing, Validation, Data curation. **Edward W. Mawji:** Writing – review & editing, Validation, Data curation. **David M. Karl:** Writing – review & editing, Validation, Data curation. **James Potemra:** Writing – review & editing, Validation, Data curation. **Fernando Santiago-Mandujano:** Writing – review & editing, Validation, Data curation. **Tetjana Ross:** Writing – review & editing, Validation, Data curation. **Kenneth L. Smith:** Writing – review & editing, Writing – original draft, Supervision, Resources, Methodology, Investigation, Funding acquisition, Formal analysis, Conceptualization.

Data and materials availability

Oxygen and other data used here are available in Dataset S1 with additional details noted in the Materials and Methods section and Ruhl et al. (2025 and refernces therein).

Declaration of competing interest

The authors declare the following financial interests/personal relationships which may be considered as potential competing interests: Thomas Soltwedel, Frank Wenzhöferreports financial support was provided by Helmholtz Centre for Ocean Research. Susan Hartman, Anita Flohr, Edward W. Mawji reports financial support was provided by Natural Environment Research Council. David Karl reports financial support was provided by National Science Foundation. If there are other authors, they declare that they have no known competing financial interests or personal relationships that could have appeared to influence the work reported in this paper.

Acknowledgments

This work was supported in part by the dedicated work of seagoing scientists and technical support teams spanning several decades and numerous ocean observing initiatives. Marguerite Blum conducted Winkler titrations, and Ed Peltzer quality-controlled Station M Winkler data from 2006 onwards. Fred Bahr contributed to Dataset S1 packaging with metadata. KLS, CLH and MM were supported by the David and Lucile Packard Foundation, including for operations at Station M. TS and FW were funded by the Helmholtz research program POF IV "Changing Earth – Sustaining our Future". Financial support for the LTER HAUSGARTEN time-series was provided by the Helmholtz infrastructure program FRAM (FRontiers in Arctic marine Monitoring). NOC authors, and work at PAP-SO, funded by Atlantic Climate and Environmental Strategic Science (AtlantiS) NERC National Capability funding (NE/

Y005589/1) and MINKE Project funded by the European Commission within the Horizon 2020 Programme (2014-2020), Grant Agreement No. 101008724. TR and the sampling, analysis and data archive of the Line P program (source of PAPA data) are supported by Fisheries and Oceans Canada. The Hawaii Ocean Time-series project has been led by R Lukas, D Karl, MJ Church and A White with funding from the National Science Foundation. DMK was funded by Grant #721252 from the Simons Foundation. The CESM 2 model output is available online through the National Center for Atmospheric Research at https://doi.org/10.26024/kgmp-c556.

Appendix A. Supplementary data

Supplementary data to this article can be found online at https://doi.org/10.1016/j.dsr.2025.104534.

References

Atlas, R., Hoffman, R.N., Ardizzone, J., Leidner, S.M., Jusem, J.C., Smith, D.K., Gombos, D., 2011. A cross-calibrated, multiplatform ocean surface wind velocity product for meteorological and oceanographic applications. Bull. Am. Meteorol. Soc. 92, 157–174. https://doi.org/10.1175/2010BAMS2946.1.

Breitburg, D., Levin, L.A., Oschlies, A., Grégoire, M., Chavez, F.P., Conley, D.J., Garçon, V., Gilbert, D., Gutiérrez, D., Isensee, K., Jacinto, G.S., 2018. Declining oxygen in the global ocean and coastal waters. Science 359 (6371), eaam7240.

Breusch, T.S., Pagan, A.R., 1979. A simple test for heteroscedasticity and random coefficient variation. Econometrica: J. Econom. Soc. 1287–1294.

Broecker, W.S., 1991. The great ocean conveyor. Oceanography (Wash. D. C.) 4 (2), 79–89.

Carpenter, J.H., 1965. The accuracy of the Winkler method for dissolved oxygen analysis. Limnol. Oceanogr. 10, 135–140.

Chiang, J.C.H., Vimont, D.J., 2004. Analogous meridional modes of atmosphere-ocean variability in the tropical Pacific and tropical Atlantic. J. Clim. 17 (21), 4143–4158.

Cianca, A., Santana, R., Hartman, S.E., Martín-González, J.M., González-Dávila, M., Rueda, M.J., Llinás, O., Neuer, S., 2013. Oxygen dynamics in the North Atlantic subtropical gyre. Deep-Sea Res. Part II Top. Stud. Oceanogr. 93, 135–147.

Cummins, P.F., Ross, T., 2020. Secular trends in water properties at Station P in the northeast Pacific: an updated analysis. Prog. Oceanogr. 186. https://doi.org/10.1016/j.pocean.2020.102329.

Danabasoglu, G., Lamarque, J.F., Bacmeister, J., Bailey, D.A., DuVivier, A.K., Edwards, J., Emmons, L.K., Fasullo, J., Garcia, R., Gettelman, A., Hannay, C., Holland, M.M., Large, W.G., Lauritzen, P.H., Lawrence, D.M., Lenaerts, J.T.M., Lindsay, K., Lipscomb, W.H., Mills, M.J., Neale, R., Oleson, K.W., Otto-Bliesner, B., Phillips, A.S., Sacks, W., Tilmes, S., van Kampenhout, L., Vertenstein, M., Bertini, A., Dennis, J., Deser, C., Fischer, C., Fox-Kemper, B., Kay, J.E., Kinnison, D., Kushner, P. J., Larson, V.E., Long, M.C., Mickelson, S., Moore, J.K., Nienhouse, E., Polvani, L., Rasch, P.J., Strand, W.G., 2020. The community Earth system model version 2 (CESM2). J. Adv. Model. Earth Syst. 12, 35. https://doi.org/10.1029/2019ms001916.

Di Lorenzo, E., Schneider, N., Cobb, K.M., Chhak, K., Franks, P.J.S., Miller, A.J., et al., 2008. North Pacific Gyre Oscillation links ocean climate and ecosystem change. Geophys. Res. Lett. 35, L08607. https://doi.org/10.1029/2007GL032838.

Dickson, R.R., Gould, W.J., Müller, T.J., Maillard, C., 1985. Estimates of the mean circulation in the deep (> 2,000 m) layer of the Eastern North Atlantic. Prog. Oceanogr. 14, 103–127.

Enfield, D.B., Mestas-Nunez, A.M., Trimble, P.J., 2001. The Atlantic Multidecadal Oscillation and its relationship to rainfall and river flows in the continental U.S. Geophys. Res. Lett. 28, 2077–2080.

Eyring, V., Bony, S., Meehl, G.A., Senior, C.A., Stevens, B., Stouffer, R.J., Taylor, K.E., 2016. Overview of the coupled model Intercomparison project phase 6 (CMIP6) experimental design and organization. Geosci. Model Dev. (GMD) 9, 1937–1958. https://doi.org/10.5194/gmd-9-1937-2016.

Feely, R., Bullister, J., Roberts, M., 1991. In: Hydrographic, Chemical and Carbon Data Obtained during the R/V Discoverer Cruise in the Pacific Ocean during WOCE Section P16N, CGC-91 (EXPOCODE 31DICGC91_2), (07 March - 07 April, 1991). US Department of Energy, Oak Ridge, Tennessee. https://doi.org/10.3334/CDIAC/otg.31DICGC91_2. http://cdiac.ornl.gov/ftp/oceans/p16nwoce/.CarbonDioxideInformationAnalysisCenter,OakRidgeNationalLaboratory.

Feely, R.A., Sabine, C.L., Millero, F.J., Dickson, A.G., Fine, R.A., Carlson, C.A., et al., 2008. Carbon dioxide, hydrographic, and chemical data obtained during the R/V Knorr repeat hydrography cruise in the Atlantic Ocean. In: Kozyr, A. (Ed.), ORNL/CDIAC-154, NDP-089. Carbon Dioxide Information Analysis Center. Oak Ridge National Laboratory, U.S. Department of Energy, Oak Ridge, Tennessee, p. 46. https://doi.org/10.3334/CDIAC/otg.nd089. CLIVAR CO2 Sections A20_2003 (22 September-20 October 2003) and A22_2003 (23 October-13 November, 2003).

Garcia-Soto, C., Cheng, L., Caesar, L., Schmidtko, S., Jewett, E.B., Cheripka, A., Abraham, J.P., 2021. An overview of ocean climate change indicators: sea surface temperature, ocean heat content, ocean pH, dissolved oxygen concentration, arctic sea ice extent, thickness and volume, sea level and strength of the AMOC (Atlantic Meridional Overturning Circulation). Front. Mar. Sci. 8, 642372. https://doi.org/10.3389/fmars.2021.642372.

Germe, A., Hirschi, J.J., Blaker, A.T., Sinha, B., 2022. Chaotic variability of the Atlantic meridional overturning circulation at subannual time scales. J. Phys. Oceanogr. 52, 929–949. https://doi.org/10.1175/JPO-D-21-0100.1.

Gordon, A.L., 1986. Interocean exchange of thermocline water. J. Geophys. Res. 91, 5037–5046.

Goyet, C., Key, R.M., Sullivan, Kevin, F., Tsuchiya, M., 1997. Carbon dioxide, hydrographic, and chemical data obtained during the R/V Thomas Washington cruise TUNES-1 in the equatorial Pacific Ocean (WOCE section P17C). ORNL/CDIAC-99, NDP-062. Carbon Dioxide Information Analysis Center. Oak Ridge National Laboratory, Oak Ridge, Tennessee. https://doi.org/10.3334/CDIAC/otg.ndp062.

Gregoire, M., Garçon, V., Garcia, H., Breitburg, D., Isensee, K., Oschlies, A., et al., 2021. A global ocean oxygen database and atlas for assessing and predicting deoxygenation and ocean health in the open and coastal ocean. Front. Mar. Sci. 8, 724913. https://doi.org/10.3389/fmars.2021.724913.

Hartman, S.E., Bett, B.J., Durden, J.M., Hanson, S.A., Iverson, M., Jeffreys, R.M., et al., 2021. Enduring science: three decades of observing the Northeast Atlantic from the porcupine abyssal plain sustained observatory (PAP-SO). Prog. Oceanogr. 191. https://doi.org/10.1016/j.pocean.2020.102508.

Hebbali, A., Hebbali, M.A., 2017. Package 'olsrr'. Version 0.5, 3.

Helm, K.P., Bindoff, N.L., Church, J.A., 2011. Observed decreases in oxygen content of the global ocean. Geophys. Res. Lett. 38 (23).

Holzer, M., DeVries, T., de Lavergne, C., 2021. Diffusion controls the ventilation of a Pacific Shadow Zone above abyssal overturning. Nat. Commun. https://doi.org/10.1038/s41467-021-24648-x.

Hogg, N.G., Biscaye, P., Gardner, W., Schmitz Jr., W.J., 1982. On the transport and modification of antarctic bottom water in the vema channel. J. Mar. Res. 40 (Suppl. l), 231–263.

Huang, B., Liu, C., Banzon, V., Freeman, E., Graham, G., Hankins, et al., 2020. Improvements of the daily optimum interpolation sea surface temperature (DOISST) version 2.1. J. Clim. 34, 2923–2939. https://doi.org/10.1175/JCLI-D-20-0166.1.

Johnson, K.M., Schneider, B., Mintrop, L., Wallace, D.W.R., 1996. Carbon dioxide, hydrographic, and chemical data obtained during the R/V meteor cruise 18/1 in the North Atlantic Ocean (WOCE section A1E, september 1991). ORNL/CDIAC-91, NDP-056. Carbon Dioxide Information Analysis Center. Oak Ridge National Laboratory, Oak Ridge, Tennessee. https://doi.org/10.3334/CDIAC/otg.ndp056.

Johnson, K., Key, R., Millero, F., Sabine, C., Wallace, D., Winn, C., et al., 2003. Carbon dioxide, hydrographic, and chemical data obtained during the R/V Knorr cruises in the North Atlantic Ocean on WOCE sections AR24. In: Kozyr, A. (Ed.), ORNL/CDIAC-143, NDP-082. Carbon Dioxide Information Analysis Center. Oak Ridge National Laboratory, U.S. Department of Energy, Oak Ridge, Tennessee. https://doi.org/10.3334/CDIAC/otg.ndp082 (November 2 - December 5, 1996) and A24, A20, and A22 (May 30 - September 3, 1997).

Johnson, G.C., 2008. Quantifying Antarctic bottom water and North Atlantic deep water volumes. J. Geophys. Res. 113, C05027. https://doi.org/10.1029/2007JC004477.

Karl, D.M., Lukas, R., 1996. The Hawaii Ocean Time-series (HOT) program: background, rationale and field implementation. Deep-Sea Res. Part II Top. Stud. Oceanogr. 43, 129–156.

Keeling, R.F., Körtzinger, A., Gruber, N., 2010. Ocean deoxygenation in a warming world. Ann. Rev. Mar. Sci 2 (1), 199–229.

Large, W.G., Pond, S., 1981. Open ocean momentum flux measurements in moderate to strong winds. J. Phys. Oceanogr. 11 (3), 324–336. https://doi.org/10.1175/1520-0485(1981)011%3C0324:OOMFMI%3E2.0.CO;2.

Long, M.C., Deutsch, C., Ito, T., 2016. Finding forced trends in oceanic oxygen. Glob. Biogeochem. Cycles 30, 381–397.

Mantua, N.J., Hare, S.R., Zhang, Y., Wallace, J.M., Francis, R.C., 1997. A Pacific interdecadal climate oscillation with impacts on salmon production. Bull. Am. Meteorol. Soc. 78, 1069–1079.

Messié, M., Ledesma, J., Kolber, D.D., Michisaki, R.P., Foley, D.G., Chavez, F.P., 2009. Potential new production estimates in four eastern boundary upwelling ecosystems. Prog. Oceanogr. 83 (1–4), 151–158. https://doi.org/10.1016/j.pocean.2009.07.018.

Nakagawa, S., Schielzeth, H., 2013. A general and simple method for obtaining R^2 from generalized linear mixed-effects models. Methods Ecol. Evol. 4 (2), 133–142.

Parsons, T.R., Maita, Y., Lalli, C.M., 1984. A Manual of Chemical and Biological Methods for Seawater Analysis. Pergamon Press, New York, p. 173.

R Core Team, 2021. R: A Language and Environment for Statistical Computing. R Foundation for Statistical Computing, Vienna, Austria. https://www.R-project.org/.

R Studio Team, 2022. RStudio: Integrated Development Environment for R.Wickham 2016.

Reid, J.L., 1997. On the total geostrophic circulation of the Pacific Ocean. Flow patterns, tracers and transports. Prog. Oceanogr. 39, 263–352.

Rodgers, K.B., Lee, S.-S., Rosenbloom, N., Timmermann, A., Danabasoglu, G., Deser, C., Edwards, J., Kim, J.-E., Simpson, I.R., Stein, K., Stuecker, M.F., Yamaguchi, R., Bódai, T., Chung, E.-S., Huang, L., Kim, W.M., Lamarque, J.-F., Lombardozzi, D.L., Wieder, W.R., Yeager, S.G., 2021. Ubiquity of human-induced changes in climate variability. Earth Syst. Dynam. 12, 1393–1411. https://doi.org/10.5194/esd-12-1393-2021.

Ross, T., Du Preez, C., Ianson, D., 2020. Rapid deep ocean deoxygenation and acidification threaten life on the Northeast Pacific seamounts. Glob. Change Biol. 26 (11), 6424–6444. https://doi.org/10.1111/gcb.15307.

Rousselet, L., Cessi, P., Forget, G., 2021. Coupling of the mid-depth and abyssal components of the global overturning circulation according to a state estimate. Sci. Adv. 7, eabf5478, 2021.

Ruhl, H.A., Ellena, J.A., Smith Jr., K.L., 2008. Connections between climate, food limitation, and carbon cycling in abyssal sediment communities: a long time-series perspective. Proc. Natl. Acad. Sci. U.S.A. 105, 17006–17011.

Ruhl, H.A., Bahr, F.L., Henson, S.A., Hosking, W.B., Espinola, B., Kahru, M., et al., 2020. Understanding the remote influences of ocean weather on the episodic pulses of particulate organic carbon flux. Deep-Sea Res. Part II Top. Stud. Oceanogr. 173, 104741.

Srokosz, M., Bryden, H., 2015. Observing the atlantic meridional overturning circulation yields a decade of inevitable surprises. Science 348. https://doi.org/10.1126/science.1255575.

Sarmiento, J.L., Hughes, T.M.C., Stouffer, R.J., Manabe, S., 1998. Simulated response of the ocean carbon cycle to anthropogenic climate warming. Nature 393, 245–249.

Sathyendranath, S., Brewin, R.J.W., Brockmann, C., Brotas, V., Calton, B., Chuprin, A., et al., 2019. An ocean-colour time-series for use in climate studies: the experience of the Ocean-Colour Climate Change Initiative (OC-CCI). Sensors 19, 4285. https://doi.org/10.3390/s19194285.

Sathyendranath, S., Jackson, T., Brockmann, C., Brotas, V., Calton, B., Chuprin, A., et al., 2021. ESA ocean colour climate change initiative (Ocean_Colour_cci): version 5.0 data. NERC EDS Centre for Environmental Data Analysis. https://doi.org/10.5285/1dbe7a109c0244aaad713e078fd3059a, 19 May 2021. https://catalogue.ceda.ac.uk/uuid/1dbe7a109c0244aaad713e078fd3059a/.

Schmidtko, S., Stramma, L., Visbeck, M., 2017. Decline in global oceanic oxygen content during the past five decades. Nature 542 (7641), 335–339.

Smith Jr., K.L., Huffard, C.L., Ruhl, H.A., 2020. Thirty-year time-series study at a station in the abyssal NE Pacific: an introduction. Deep-Sea Res. Part II Top. Stud. Oceanogr. 173. https://doi.org/10.1016/j.dsr2.2020.104764.

Smith Jr., K.L., Messie, M., Connolly, T.P., Huffard, C.L., 2022. Decadal time-series depletion of dissolved oxygen at abyssal depths in the Northeast Pacific. Geophys. Res. Lett. 49, e2022GL101018.

Smith Jr., K.L., Ruhl, H.A., Huffard, C.L., Messié, M., Kahru, M., 2018. Surface ocean to abyssal depth carbon cycling in the NE Pacific; underestimated pulse events during long time-series. Proceedings of the National Academy of Sciences, USA 115 (48), 12235–12240.

Smith Jr., K.L., Ruhl, H.A., Kaufmann, R.S., Kahru, M., 2008. Tracing abyssal food supply back to upper-ocean processes over a 17-year time-series in the northeast Pacific. Limnol. Oceanogr. 53, 2655–2667.

Soltwedel, T., Bauerfeind, E., Bergmann, M., Bracher, A., Budaeva, N., Busch, K., et al., 2016. Natural variability or anthropogenically-induced variation? Insights from 15 years of multidisciplinary observations at the arctic open-ocean LTER site HAUSGARTEN. Ecol. Indic. 65, 89–102. https://doi.org/10.1016/j.ecolind.2015.10.001.

Steinberg, D.K., Carlson, C.A., Bates, N.R., Johnson, R.J., Michaels, A.F., Knap, A.H., 2001. Overview of the US JGOFS Bermuda Atlantic Time-series Study (BATS): a decade-scale look at ocean biology and biogeochemistry. Deep-Sea Research II 48, 1405–1447.

Talley, L.D., 2013. Closure of the global overturning circulation through the Indian, pacific, and southern oceans. Oceanography (Wash. D. C.) 26 (1), 80–97.

van Aken, H.M., 2000. The hydrography of the mid-latitude northeast Atlantic Ocean: I: the deep water masses. Deep-Sea Res. Part I Oceanogr. Res. Pap. 47 (5), 757–788.

Wentz, F.J., Scott, J., Hoffman, R., Leidner, M., Atlas, R., Ardizzone, J., 2015. Remote Sensing Systems Cross-Calibrated Multi-Platform (CCMP) 6-hourly Ocean Vector Wind Analysis Product on 0.25 Deg Grid, Version 2.0. Remote Sensing Systems, Santa Rosa, CA. Available online at www.remss.com/measurements/ccmp. Accessed 06/13/2022.

Wolter, K., Timlin, M.S., 1993. Monitoring ENSO in COADS with a seasonally adjusted principal component index. Proc. Of the 17th Climate Diagnostics Workshop, Norman, OK, NOAA/NMC/CAC, NSSL, Oklahoma Clim. Survey, CIMMS and the School of Meteor. Univ. of Oklahoma, pp. 52–57.

Wong, C.S., Garrett, J., Freeland, H., 1994. Hydrographic, chemical and carbon data obtained during the R/V john P. Tully cruise in the Pacific Ocean during WOCE section P15N (EXPOCODE 18dd9403/1,2) (06 September - 10 November, 1994). US Department of Energy, Oak Ridge, Tennessee. https://doi.org/10.3334/CDIAC/otg.18DD9403_1_2. http://cdiac.ornl.gov/ftp/oceans/p15nabwoce/.CarbonDioxideInformationAnalysisCenter,OakRidgeNationalLaboratory.

Ruhl, H., Huffard, C., Messié, M., Connolly, T., Soltwedel, T., Wenzhöfer, F., Johnson, R., Bates, N.R., Hartman, S., Flohr, A., Mawji, E., Karl, D.M., Potemra, J., Santiago-Mandujano, F., Ross, T., Smith, K.L., 2025. Decadal change in deep-ocean dissolved oxygen in the North Atlantic Ocean and North Pacific Ocean [Data set]. In Deep-Sea Research, Part 1. Zenodo. https://doi.org/10.5281/zenodo.15699979.